

Universal Segmentation of 33 Anatomies

Pengbo Liu², Yang Deng¹, Ce Wang², Yuan Hui², Qian Li², Jun Li², Shiwei Luo⁴, Mengke Sun², Quan Quan², Shuxin Yang², You Hao², Honghu Xiao³,
Chunpeng Zhao³, Xinbao Wu³, and S. Kevin Zhou^{1,2}

¹ School of Biomedical Engineering & Suzhou Institute for Advanced Research
Center for Medical Imaging, Robotics, and Analytic Computing & Learning
(MIRACLE) University of Science and Technology of China, Suzhou 215123, China

² Key Lab of Intelligent Information Processing of Chinese Academy of Sciences
(CAS), Institute of Computing Technology, CAS, Beijing, 100190, China
liupengbo2019@ict.ac.cn

³ Beijing Jishuitan Hospital, Beijing 100035, China

⁴ Department of Radiology, Guangzhou First People’s Hospital, School of Medicine,
South China University of Technology, Guangzhou, China

Abstract. In the paper, we present an approach for learning a single model that universally segments 33 anatomical structures, including vertebrae, pelvic bones, and abdominal organs. Our model building has to address the following challenges. Firstly, while it is ideal to learn such a model from a large-scale, fully-annotated dataset, it is practically hard to curate such a dataset. Thus, we resort to learn from a union of multiple datasets, with each dataset containing the images that are partially labeled. Secondly, along the line of partial labelling, we contribute an open-source, large-scale vertebra segmentation dataset for the benefit of spine analysis community, **CTSpine1K**, boasting over 1,000 3D volumes and over 11K annotated vertebrae. Thirdly, in a 3D medical image segmentation task, due to the limitation of GPU memory, we always train a model using cropped patches as inputs instead a whole 3D volume, which limits the amount of contextual information to be learned. To this, we propose a **cross-patch transformer** module to fuse more information in adjacent patches, which enlarges the aggregated receptive field for improved segmentation performance. This is especially important for segmenting, say, the elongated spine. Based on 7 partially labeled datasets that collectively contain about 2,800 3D volumes, we successfully learn such a universal model. Finally, we evaluate the universal model on multiple open-source datasets, proving that our model has a good generalization performance and can potentially serve as a solid foundation for downstream tasks.

Keywords: Universal segmentation model · CTSpine1K dataset · Cross-patch transformer · Partially labeled datasets.

1 Introduction

Medical image segmentation [19, 20] is a fundamental task in clinical workflow, which allows intelligent systems to know where the boundaries of target struc-

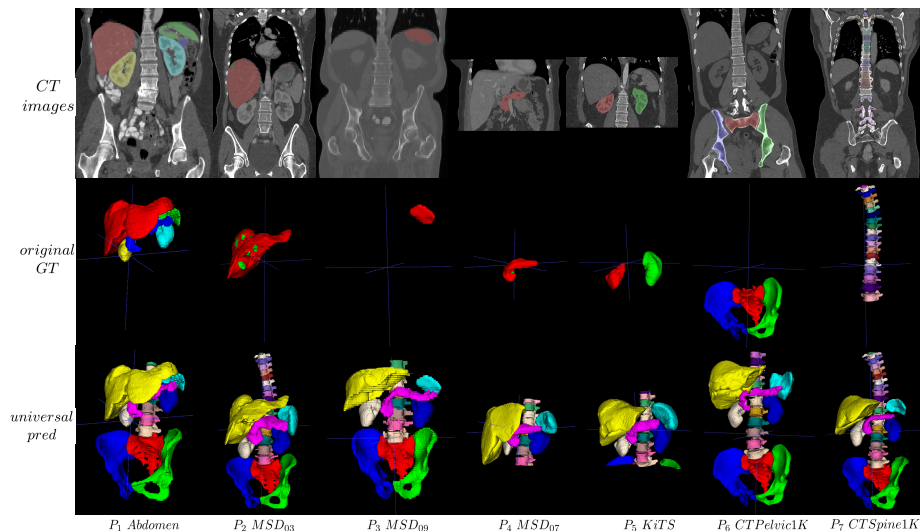


Fig. 1. CT image examples of seven partially labeled datasets. 1st row shows the coronal view of CT images overlapped with original ground truth. 2nd row shows the 3D rendering of original ground truth. 3rd row shows the 3D rendering of results predicted from our 33-anatomy universal segmentation model.

tures are. The more structures, the better. But it is practically hard to curate a large-scale, fully-annotated dataset, from which a model that segments myriad anatomies is learned, as annotating all anatomies of interest needs a support of professional knowledge from different doctors, and it is expensive and time-consuming. Fortunately, there exists medical image datasets which are partially labeled according to the task at the time. As shown in the 1st and 2nd rows of Fig. 1, each dataset only contains the labels of a part of anatomies. Fusing these partially-labeled datasets together is a promising direction. Some methods [3, 13, 17, 21] have been proposed, verifying that such learned model outperforms the models that are individually trained from a single dataset. However, these methods deal with only abdominal organs with limited field-of-view (FOV).

On the other hand, although constructing open source datasets is a toilsome task, there are some recent datasets with a noticeable scale [9, 10]. Ma *et al.* [10] curate a multi-organ segmentation dataset of over 1,000 volumes from 12 sites with five abdominal organs completely labeled. The same goes for pelvic bone segmentation, too. Liu *et al.* [9] construct a large-scale dataset containing over 1,000 volumes of pelvic bone structures.

In this paper, we are interested in segmenting both the bones (spine and pelvis) and organs simultaneously. While there are sizeable organ datasets [6, 14] by now, there is a lack of sizeable bone datasets. Schnider *et al.* [11] segment 125 distinct bones in the upper-body CT, but with only 5 annotated cases. Pelvis and spine are important structures maintaining the stability of the body. The dataset

gap in pelvic bone segmentation has been filled by Liu *et al.* [9], but the gap in vertebrae segmentation has not yet filled. For vertebrae segmentation, the Verse challenge is a famous benchmark, but only 141 labeled cases for training [12]. To this, we hereby curate images from many sources to construct a large-scale dataset, called **CTSpine1K**, containing 1,003 3D CT images and with over 11K vertebrae segmentation annotations. We will open source CTSpine1K.

Learning to segmenting the elongated spine and its associated vertebrae is challenged by the limited GPU memory. It is conventional to train a model using cropped patches as inputs instead a whole 3D volume, which limits the amount of contextual information to be learned. To this, we propose a **cross-patch transformer** module to fuse more information in adjacent patches, which enlarges the aggregated receptive field for improved segmentation performance.

After CTSpine1K is built, we learn a universal model for segmentation of *33 categories anatomies* from 7 partially-labeled datasets with about 2,800 volumes. The 33 anatomies include 3 pelvic bone, 5 abdomen organs, and 25 vertebrae. We verify the generalization performance of our model on three open source datasets. We will make this universal model public too to benefit the community.

Our contributions can be summarized as:

- We propose and will open source an *universal model for segmentation of 33 anatomies* trained on 7 partially labeled datasets with about 2,800 volumes. Its generalization capability has been verified in other open source datasets.
- For vertebrae segmentation, we construct a large-scale CT dataset, *CT-Spine1K*, with 1,003 3D CT images and over 11K vertebrae segmentation annotations, to benefit the spine analysis community.
- For spine segmentation of CTSpine1K, we also propose a *cross-patch transformer module* (CPTM) to catch more long-range contextual information to improve the accuracy of identification of vertebrae.

2 Method

2.1 Cross-patch transformer

Due to the large volume size and limited GPU memory, patch-based method is a normal training paradigm in 3D medical image segmentation. This limits the receptive field of the model fundamentally. For example, when the patch size is $(128 \times 128 \times 128)$, the information can be caught is limited this patch size, regardless of the depth of the model. But for spine modeling, long-range contextual information is important for identification of vertebrae. Although transformer [15] is famous at fusing long-range information in computer vision, there is no long-range information to catch in a single patch [5, 16].

We propose a cross-patch transformer module for modeling long-range context. As shown in Fig. 2 (a), we crop three patches consecutively with $(64 \times 128 \times 128)$ overlap as input. Then we can equivalently supply a ‘merged patch’ with a double size of $(256 \times 128 \times 128)$ to the model. A shared encoder is used to extract information from each of three patches, respectively. Then the flattened feature

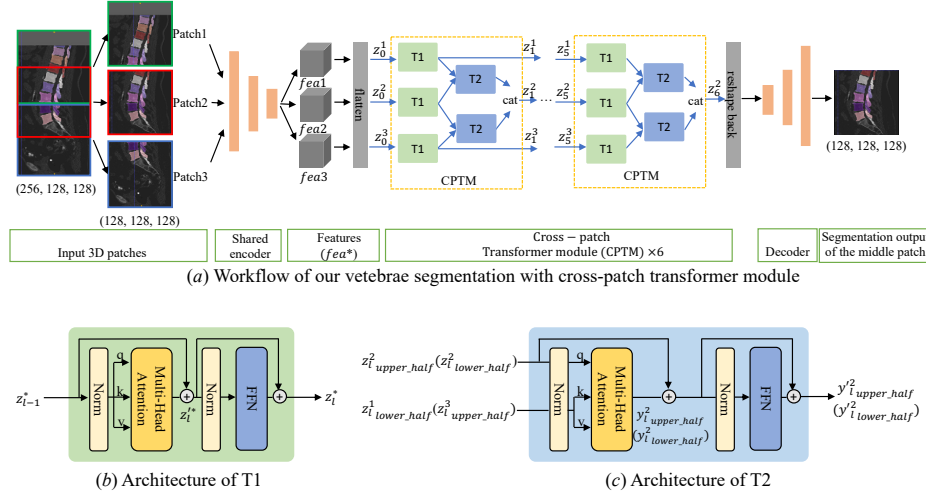


Fig. 2. (a) The overview of our spine segmentation workflow. The inputs are three consecutive 3D patches with overlapping. After being encoded by a shared encoder, the features of three patches are fused by a series of CPTMs. In each CPTM, T_1 and T_2 are used to extract information within one patch and fuse information between two patches, respectively. Then all contextual information is merged to the middle patch for final segmentation. (b) and (c) show the structure of the T_1 and T_2 , respectively.

maps are sent to a series of CPTMs for information fusion. All information of this double-sized ‘patch’ is merged into the middle patch, which is decoded for the prediction of the segmentation.

In our CPTM, there are two kinds of transformer blocks, T_1 and T_2 . T_1 follows a normal transformer mechanism, as shown in Fig. 2 (b) and Eq. (1), fusing global information within a single input patch. Mathematically,

$$z_i^* = MSA(LN(z_{i-1}^*)) + z_{i-1}^*, \quad z_i^* = FFN(LN(z_i^*)) + z_i^*, \quad (1)$$

where z_{i-1}^* , z_i^* are input and output features, respectively. MSA is multi-head attention, LN is layer normalization, and FFN is feed-forward network.

T_2 is used to fuse information from two adjacent patches (the top ‘Patch1’ and the bottom ‘Patch3’) with that of the middle ‘Patch2’. The fusion proceeds as shown in Fig. 2 (c). First, it integrates the features of the intersection parts of two patches (say the lower half of ‘Patch1’ and the upper half of ‘Patch2’ or similarly the lower half of ‘Patch2’ and the upper half of ‘Patch3’) using Eq. (2) to (4). Then, we concatenate the integrated features back to a whole patch. This way, the information of three patches is merged together to the middle patch.

$$y_l^2{}_{upper_half} = MSA(LN(z_l^2{}_{upper_half}), LN(z_l^1{}_{lower_half})) + z_l^2{}_{upper_half}, \quad (2)$$

$$y_l^2{}_{upper_half} = FFN(LN(y_l^2{}_{upper_half})) + y_l^2{}_{upper_half}, \quad (3)$$

$$z_l^2 = torch.cat(y_l^2{}_{upper_half}, y_l^2{}_{lower_half}). \quad (4)$$

Table 1. A summary of 7 training & validation datasets and 4 independent testing datasets used in our experiments.

Phase	Datasets	Modality	# of labeled volumes	Annotated organs	Mean spacing (z, y, x)	Source
Training & Validation	Dataset1 (P_1)	CT	30	Five organs	(0.76, 0.76, 3.0)	Abdomen in [2]
	Dataset2 (P_2)	CT	131	Liver	(0.77, 0.77, 1.0)	MSD_Liver [14]
	Dataset3 (P_3)	CT	41	Spleen	(0.79, 0.79, 1.6)	MSD_Spleen [14]
	Dataset4 (P_4)	CT	281	Pancreas	(0.80, 0.80, 2.5)	MSD_Pancreas [14]
	Dataset5 (P_5)	CT	210	L&R Kidneys	(0.78, 0.78, 0.8)	KiTS [6]
	Dataset6 (P_6)	CT	1109	Pelvic Bones	(0.78, 0.78, 1.5)	CTPelvic1K [2]
	Dataset7 (P_7)	CT	1005	Vertebrae	(0.76, 0.76, 1.1)	CTSpine1K (<i>Ours</i>)
	All	CT	2807	Bones & organs	(0.77, 0.77, 1.4)	-
Testing	Amos	CT	200	Five organs	(0.74, 0.74, 5.0)	Coming soon
	CLINIC	CT	200	Five organs	(0.74, 0.74, 1.2)	In-house
	Verse19	CT	80/40/40	Vertebrae	(1.00, 1.00, 1.6)	Challenge [12]
	Verse20	CT	120/103/103	Vertebrae	(0.80, 0.80, 1.4)	Challenge [12]

2.2 Pseudo label prediction and universal model learning

Learning from predicted pseudo labels is a simple but efficient semi-supervised method. Because the structures of humans are similar, in addition to the annotations that already exist in the partially labeled datasets, there also exists *a large amount of unlabeled anatomies* in images waiting to be mined and utilized.

To construct a universal model to segment organs and bones, we curate 7 partially labeled datasets, and train three models separated based on the SOTA methods for organs [13], pelvic bones [7], and vertebrae (with CPTM in 2.1), respectively. Then we predict all 33 anatomies for all images in these 7 partially labeled datasets as pseudo labels, which are replaced by original ground truth labels if present, constructing a 33 classes ‘fully labeled’ segmentation dataset. Finally, we train a 33-anatomy segmentation model using nnU-Net [7].

3 Experiments

3.1 Datasets

In this part, we introduce the datasets used in our experiments, including CT-Spine1K we construct. Table 1 provides a summary of these datasets.

CTSpine1K Dataset To build a comprehensive spine dataset that replicates practical appearance variations, we curate a large-scale dataset of CT images that contain spinal vertebrae from the following four open sources: COLONOG [8], HNSCC-3DCT-RT [1], MSD T10 [14], and COVID-19 [4].

We reformat all DICOM images to NIFTI to simplify data processing and de-identify images to meet the institutional review board (IRB) policies of contributing sites. All existing sub-datasets are under Creative Commons license CC-BY-NC-SA and we will keep the license unchanged. For sub-dataset MSD T10 and sub-dataset COVID-19, we choose some cases from them, and in all these data sources, we exclude those cases of very low quality. The overview of our dataset can be seen in Table 2. The details about the CTSpine1K dataset and the annotation pipeline could be seen in supplementary material.

Table 2. Overview of our large-scale CTSpine1K dataset. Ticks[✓] in the table refer to that this dataset contains some special cases with sacral lumbarization or lumbar sacralization and we will list their IDs in the open source. We exclude the metal-artifact cases due to the difficulty of labeling them.

Dataset name	Cases	# of vertebrae	Mean spacing(mm)	Mean size	Source and Year
COLONOG [✓]	784	Thoracic and lumbar vertebrae (8,136)	(0.75, 0.75, 0.8)	(512, 512, 542)	[8] 2008
HNSCC-3DCT-RT	31	Cervical and thoracic vertebrae (450)	(1.09, 1.09, 2.0)	(512, 512, 202)	[1] 2018
MSD T10 [✓]	148	Thoracic and lumbar vertebrae (2,101)	(0.78, 0.78, 1.6)	(512, 512, 458)	[14] 2019
COVID-19	40	Cervical and thoracic vertebrae (612)	(0.79, 0.79, 4.5)	(512, 512, 93)	[4] 2020
CTSpine1K [✓]	1,003	Cervical, thoracic and lumbar vertebrae (11,299)	(0.77, 0.77, 1.1)	(512, 512, 501)	-

Other datasets The other 6 partially labeled datasets in training phase are: CTPelvic1K [9], MSD_Liver [14], MSD_Spleen [14], MSD_Pancreas [14], KiTS [6], and Abdomen [2]. The details are shown in Table 1. Different from CTSpine1K, we split these 6 datasets into training: testing with ratio of 4 : 1, respectively. For fair model selection, we choice the model saved in the last epoch.

We also leverage 4 independent testing datasets to verify the generalization capacity of our universal model: Amos, CLINIC, Verse19 [12], and Verse20 [12]. Amos is temporarily private, and will open source soon. CLINIC is an in-house dataset by now.

3.2 Results and discussion

Evaluation metrics To evaluate the performance of different methods, we employ widely-used segmentation metrics, including *Dice coefficient (DC)* and *Hausdorff distance (HD)*. For organs evaluation, we use the 95th percentile HD (HD95) to measure the degree of false positive prediction. Due to the computing pressure and referring to challenge Verse19 and Verse20, for bones evaluation, we use HD instead, equipped with maximum connected region post-processing to prevent influence of outlier. In addition, to evaluate the performance of vertebrae localization [12], we also compute the *Identification Rate (id.rate)* and *Localization distance (d_{mean})*. Because there is no landmark detection output from our segmentation model, we define the centroid of each vertebra as a landmark.

Cross-patch transformer module (CPTM) Validation results of models trained separately for different part of anatomies are shown in Table 3. For vertebrae segmentation in CTSpine1K, we implement current SOTA CNN-based and transformer-based methods [7, 18] to find a more powerful model to supply more precise pseudo label for next stage of universal model training. We find that nnU-Net can keep more stable performance in different scenarios, so we deploy our CPTM into nnU-Net framework. There is only slight improvement on DC compared with nnU-Net, but in Table 4 we find CPTM can improve

Table 3. The average DC and HD results for different methods, validated on different partially labeled datasets. [S] means separately trained model for specific task, i.e., pelvic bone, organs, and vertebrae segmentation. [Uni] means an universal model trained for 33 categories via pseudo label method with all partially labeled datasets. The number in [] means how many classes in that structure. [(6)] and [(25)] mean that #25 vertebra is included. ‘-’ means no result to show.

Structures [#ofclasses]	[S]nnU-Net [7]		[S]MargExc [13]		[S]nnFormer [18]		[S]nnU-Net [7]		[S]CPTM		[Uni] Ours	
	DC	HD	DC	HD	DC	HD	DC	HD	DC	HD	DC	HD
Pelvic bones mean [3]	.971	5.78	-	-	-	-	-	-	-	-	.973	6.23
Organs mean [5]	-	-	.942	3.67	-	-	-	-	-	-	.942	2.55
Cervical V [7]	-	-	-	-	.626	9.94	.816	7.76	.807	8.38	.831	7.19
Thoracic V [12]	-	-	-	-	.806	12.44	.870	9.97	.880	9.68	.884	9.38
Lumbar V [5]	-	-	-	-	.906	11.72	.933	8.36	.935	8.26	.934	8.18
Lumbar V [(6)]	-	-	-	-	.755	11.72	.816	8.59	.818	8.41	.817	11.65
All V mean [24]	-	-	-	-	.774	11.56	.867	8.99	.870	9.01	.879	8.49
All V mean [(25)]	-	-	-	-	.743	11.56	.842	9.02	.845	9.03	.853	9.31

Table 4. The performance of landmark localization of different segmentation models under the newly defined landmark (3.2). HNSCC-3DCT-RT, MSD T10, COVID-19, and COLONOG are different sources in CTSpine1K dataset. *id.rate* is reported in % and *d_{mean}* in mm.

Vertebrae source	# of Scans	[S]nnFormer [18]		[S]nnU-Net [7]		[S]CPTM		[Uni]nnU-Net	
		<i>id.rate</i>	<i>d_{mean}</i>	<i>id.rate</i>	<i>d_{mean}</i>	<i>id.rate</i>	<i>d_{mean}</i>	<i>id.rate</i>	<i>d_{mean}</i>
HNSCC-3DCT-RT	5+5	98.38	1.93	98.18	1.37	100	0.87	100	0.67
MSD T10	30+30	95.44	2.11	97.05	1.42	97.90	1.21	97.31	1.29
COVID-19	10+10	94.60	2.75	98.28	1.22	98.92	1.01	97.23	1.49
COLONOG	152+152	96.80	1.46	96.61	1.38	96.51	1.36	97.18	1.19
All	197+197	96.52	1.64	96.80	1.37	96.90	1.31	97.27	1.20

vertebrae identification rate obviously. This means the CPTM can fuse more useful context to enhance the performance of segmentation. Experiment of nnU-Net trained on same size input of CPTM is not implemented because of the limit of GPU memory.

Universal model Considering the wide range of applications of nnU-Net [7], we train our universal model based on it. On validation set, as shown in Table 3 and Table 4, there is an obvious improvement on vertebrae segmentation. For pelvic bones and five organs segmentation, existing methods [7, 13] have almost reached the upper bound performance, so there is not very obvious improvements on pelvic bones and organs segmentation.

More importantly, we verify the generalization capacity of our universal model on other testing datasets, which are never seen in the training phase. As shown in Table 5, when we deploy our universal model directly for testing organs segmentation, we can achieve the improvement of 2.5 and 2.0 in Dice and of 35.7% and 23.5% in HD95 on Amos and CLINIC datasets, respectively. For vertebrae segmentation, we choose two famous challenges [12], Verse19 and Verse20, for testing our model’s generalization performance. In Table 5, to compare with

Table 5. Generalization performance of our universal model on other testing datasets. ‘f.t.’ means ‘finetuned to’. ‘f.t.s’ means ‘from the scratch’. *id.rate* is reported in % and *d_{mean}* in mm. Attention: in SOTA method of [12], the landmark definition are different.

Vertebrae	# of Scans	[S]MargExc [13]				[S]Verse19 f.t.s [7]				[S]Verse20 f.t.s [7]			
		DC	HD	<i>id.rate</i>	<i>d_{mean}</i>	DC	HD	<i>id.rate</i>	<i>d_{mean}</i>	DC	HD	<i>id.rate</i>	<i>d_{mean}</i>
Amos	200	.855	10.20	-	-	-	-	-	-	-	-	-	-
CLINIC	107	.934	3.23	-	-	-	-	-	-	-	-	-	-
Verse19 val	40	-	-	-	-	.857	14.95	92.9	3.11	-	-	-	-
Verse19 test	40	-	-	-	-	.863	27.21	92.9	3.16	-	-	-	-
Verse20 val	103	-	-	-	-	-	-	-	-	.805	34.38	87.9	4.72
Verse20 test	103	-	-	-	-	-	-	-	-	.829	29.07	89.9	3.98

Vertebrae	# of Scans	[Uni]nnU-Net				[Uni] f.t. Verse19				[Uni] f.t. Verse20				SOTA in [12]			
		DC	HD	<i>id.rate</i>	<i>d_{mean}</i>	DC	HD	<i>id.rate</i>	<i>d_{mean}</i>	DC	HD	<i>id.rate</i>	<i>d_{mean}</i>	DC	HD	<i>id.rate</i>	<i>d_{mean}</i>
Amos	200	.880	6.56	-	-	-	-	-	-	-	-	-	-	-	-	-	-
CLINIC	107	.954	2.47	-	-	-	-	-	-	-	-	-	-	-	-	-	-
Verse19 val	40	.808	18.64	89.0	3.31	.914	9.40	99.7	0.91	-	-	-	-	.909	6.35	95.7	4.27
Verse19 test	40	.829	17.08	93.4	3.56	.904	10.28	96.8	1.55	-	-	-	-	.898	7.08	94.3	4.80
Verse20 val	103	.797	32.08	87.5	4.69	-	-	-	-	.834	18.41	89.4	4.01	.917	5.80	95.1	2.90
Verse20 test	103	.824	26.40	91.5	3.54	-	-	-	-	.866	18.03	93.2	2.59	.897	6.06	92.8	2.91

SOTA methods in these two challenges, we modify the evaluation metric of DC and HD from vertebra-level to patient-level, referring to [12], without post-processing. When we directly test on validation and testing set of Verse19 and Verse20, the performance on Verse19 is not good compared with model trained from scratch. But after finetuning on training set, our model’s performance gets a big improvement. The performance on verse19 surpasses the SOTA method, which have a complicated three stage design [12]. The performance on verse20 also gets a big boost after finetuning on training dataset. For pelvic bone segmentation, there is no large scale open source datasets to test.

For the visualization of segmentation results of our universal model, please refer to the 3rd row in Fig. 1. The 33 anatomies can be predicted by only one inference, a feat never realized before.

4 Conclusion

In this paper, to solve the problem that a large-scale, fully-labeled dataset in medical image segmentation is difficult to obtain then a robust model cannot reliably be trained, we fuse 7 partially labeled datasets based on pseudo label method to train a 33-class segmentation model. Because the structure of the human body is similar, our method can effectively unleash the potential of a large amount of unlabeled data in partially labeled datasets. This universal 33-class segmentation model has good generalization performance and can also be used as a pretrained model to benefit subsequent tasks. Among them, a large-scale vertebrae segmentation dataset is constructed by us, CTSpine1K, containing 1,003 3D CT images and over 10k vertebrae annotations, which effectively fill the gap of data insufficiency in spine analysis. To account for the elongated nature of a spine, we also propose a cross-patch transformer module (CPTM) to improve the accuracy of vertebrae identification. Both the 33-anatomy universal segmentation model and the CTSpine1K dataset will be open source. We plan to keep building a universal model to include more anatomies in future.

References

1. Bejarano, T., De Ornelas Couto, M., Mihaylov, I.: Head-and-neck squamous cell carcinoma patients with ct taken during pre-treatment, mid-treatment, and post-treatment dataset. the cancer imaging archive; 2018
2. Bennett, L., Zhoubing, X., Juan, Eugenio, I., Martin, S., Thomas, Robin, L., Arno, K.: 2015 miccai multi-atlas labeling beyond the cranial vault – workshop and challenge (2015). <https://doi.org/10.7303/syn3193805>
3. Fang, X., Yan, P.: Multi-organ segmentation over partially labeled datasets with multi-scale feature abstraction. *IEEE Transactions on Medical Imaging* **39**(11), 3619–3629 (2020)
4. Harmon, S.A., Sanford, T.H., Xu, S., Turkbey, E.B., Roth, H., Xu, Z., Yang, D., Myronenko, A., Anderson, V., Amalou, A., et al.: Artificial intelligence for the detection of covid-19 pneumonia on chest ct using multinational datasets. *Nature communications* **11**(1), 1–7 (2020)
5. Hatamizadeh, A., Tang, Y., Nath, V., Yang, D., Myronenko, A., Landman, B., Roth, H.R., Xu, D.: Unetr: Transformers for 3d medical image segmentation. In: *Proceedings of the IEEE/CVF Winter Conference on Applications of Computer Vision*. pp. 574–584 (2022)
6. Heller, N., Sathianathen, N., Kalapara, A., Walczak, E., Moore, K., Kaluzniak, H., Rosenberg, J., Blake, P., Rengel, Z., Oestreich, M., Dean, J., Tradewell, M., Shah, A., Tejjpaul, R., Edgerton, Z., Peterson, M., Raza, S., Regmi, S., Papanikolopoulos, N., Weight, C.: The kits19 challenge data: 300 kidney tumor cases with clinical context, CT semantic segmentations, and surgical outcomes. arXiv:1904.00445 (2019)
7. Isensee, F., Jaeger, P.F., Kohl, S.A., Petersen, J., Maier-Hein, K.H.: nnu-net: a self-configuring method for deep learning-based biomedical image segmentation. *Nature Methods* **18**(2), 203–211 (2021)
8. Johnson, C.D., Chen, M.H., Toledano, A.Y., Heiken, J.P., Dachman, A., Kuo, M.D., Menias, C.O., Siewert, B., Cheema, J.I., Obregon, R.G., et al.: Accuracy of ct colonography for detection of large adenomas and cancers. *New England Journal of Medicine* **359**(12), 1207–1217 (2008)
9. Liu, P., Han, H., Du, Y., Zhu, H., Li, Y., Gu, F., Xiao, H., Li, J., Zhao, C., Xiao, L., et al.: Deep learning to segment pelvic bones: large-scale ct datasets and baseline models. *International Journal of Computer Assisted Radiology and Surgery* **16**(5), 749–756 (2021)
10. Ma, J., Zhang, Y., Gu, S., Zhu, C., Ge, C., Zhang, Y., An, X., Wang, C., Wang, Q., Liu, X., Cao, S., Zhang, Q., Liu, S., Wang, Y., Li, Y., He, J., Yang, X.: Abdomenct-1k: Is abdominal organ segmentation a solved problem. *IEEE Transactions on Pattern Analysis and Machine Intelligence* pp. 1–1 (2021). <https://doi.org/10.1109/TPAMI.2021.3100536>
11. Schnider, E., Horváth, A., Rauter, G., Zam, A., Müller-Gerbl, M., Cattin, P.C.: 3d segmentation networks for excessive numbers of classes: distinct bone segmentation in upper bodies. In: *International Workshop on Machine Learning in Medical Imaging*. pp. 40–49. Springer (2020)
12. Sekuboyina, A., Hussein, M.E., Bayat, A., Löffler, M., Liebl, H., Li, H., Tetteh, G., Kukačka, J., Payer, C., Štern, D., et al.: Verse: a vertebrae labelling and segmentation benchmark for multi-detector ct images. *Medical image analysis* **73**, 102166 (2021)
13. Shi, G., Xiao, L., Chen, Y., Zhou, S.K.: Marginal loss and exclusion loss for partially supervised multi-organ segmentation. *Medical Image Analysis* p. 101979 (2021)

14. Simpson, A.L., Antonelli, M., Bakas, S., Bilello, M., Farahani, K., Van Ginneken, B., Kopp-Schneider, A., Landman, B.A., Litjens, G., Menze, B., Ronneberger, O., Summers, R.M., Bilic, P., Christ, P.F., Do, R.K., Gollub, M., Golia-Pernicka, J., Heckers, S.H., Jarnagin, W.R., McHugo, M.K., Napel, S., Vorontsov, E., Maier-Hein, L., Cardoso, M.J.: A large annotated medical image dataset for the development and evaluation of segmentation algorithms. arXiv:1902.09063 (2019)
15. Vaswani, A., Shazeer, N., Parmar, N., Uszkoreit, J., Jones, L., Gomez, A.N., Kaiser, L., Polosukhin, I.: Attention is all you need. *Advances in neural information processing systems* **30** (2017)
16. Xia, Y., Yao, J., Lu, L., Huang, L., Xie, G., Xiao, J., Yuille, A., Cao, K., Zhang, L.: Effective pancreatic cancer screening on non-contrast ct scans via anatomy-aware transformers. In: *International Conference on Medical Image Computing and Computer-Assisted Intervention*. pp. 259–269. Springer (2021)
17. Zhang, J., Xie, Y., Xia, Y., Shen, C.: Dodnet: Learning to segment multi-organ and tumors from multiple partially labeled datasets. In: *Proceedings of the IEEE/CVF Conference on Computer Vision and Pattern Recognition*. pp. 1195–1204 (2021)
18. Zhou, H.Y., Guo, J., Zhang, Y., Yu, L., Wang, L., Yu, Y.: nnformer: Interleaved transformer for volumetric segmentation. arXiv preprint arXiv:2109.03201 (2021)
19. Zhou, S.K., Greenspan, H., Davatzikos, C., Duncan, J.S., van Ginneken, B., Madabhushi, A., Prince, J.L., Rueckert, D., Summers, R.M.: A review of deep learning in medical imaging: Imaging traits, technology trends, case studies with progress highlights, and future promises. *Proceedings of the IEEE* (2021)
20. Zhou, S.K., Rueckert, D., Fichtinger, G.: *Handbook of Medical Image Computing and Computer Assisted Intervention*. Academic Press (2019)
21. Zhou, Y., Li, Z., Bai, S., Wang, C., Chen, X., Han, M., Fishman, E., Yuille, A.L.: Prior-aware neural network for partially-supervised multi-organ segmentation. In: *Proceedings of the IEEE/CVF International Conference on Computer Vision*. pp. 10672–10681 (2019)